

UCRL-96498
PREPRINT

**Shock-Wave Studies Using Plastic Flyers
Driven by an Electric Gun for
Hypervelocity Impact on
Selected Materials**

J. E. Osher, H. H. Chau, G. R. Gathers,
R. S. Lee, G. W. Pomykal, and R. C. Weingart

This paper was prepared for submittal to
*Proceedings of the APS 1987 Topical
Conference on Shock Waves in Condensed Matter,
Monterey, California, July 20-23, 1987*

June 1987

CIRCULATION COPY
SUBJECT TO RECALL
IN TWO WEEKS

Lawrence
Livermore
National
Laboratory

This is a preprint of a paper intended for publication in a journal or proceedings. Since changes may be made before publication, this preprint is made available with the understanding that it will not be cited or reproduced without the permission of the author.

DISCLAIMER

This document was prepared as an account of work sponsored by an agency of the United States Government. Neither the United States Government nor the University of California nor any of their employees, makes any warranty, express or implied, or assumes any legal liability or responsibility for the accuracy, completeness, or usefulness of any information, apparatus, product, or process disclosed, or represents that its use would not infringe privately owned rights. Reference herein to any specific commercial products, process, or service by trade name, trademark, manufacturer, or otherwise, does not necessarily constitute or imply its endorsement, recommendation, or favoring by the United States Government or the University of California. The views and opinions of authors expressed herein do not necessarily state or reflect those of the United States Government or the University of California, and shall not be used for advertising or product endorsement purposes.

SHOCK-WAVE STUDIES USING PLASTIC FLYERS DRIVEN BY AN ELECTRIC GUN FOR HYPERVELOCITY IMPACT ON SELECTED MATERIALS

J. E. Osher, H. H. Chau, G. R. Gathers, R. S. Lee, G. W. Pomykal, and R. C. Weingart

Lawrence Livermore National Laboratory, P.O. Box 808, Livermore, CA 94550*

The Lawrence Livermore National Laboratory (LLNL) electric gun is in use for a variety of shock-wave studies using plastic flyer impact on simple materials such as 6061-T6 Al and selected composite combinations at both normal and oblique incidence. The most commonly used flyer is 0.3-mm-thick Kapton at velocities from 1 to 18 mm/ μ s. The experimentally measured wave shapes and attenuation are compared to code calculations, with particular interest in spall threshold and coupled momentum.

1. INTRODUCTION

The study of shock-wave phenomena generally requires a source to launch a wave of interest; diagnostics to characterize the wave and its interaction with material; and recovery, if possible, of the test specimen in its final state. We will describe shock-wave studies using the LLNL 100-kV electric gun to accelerate flat-plate flyers of thin plastic weighing from 4.3 to 0.043 g to impact on selected materials at impulse densities over the range of 1 to 80 ktaps (tap is the generally accepted unit of impulse or momentum/unit area in g/(cm \times s)).

1.1. Electric gun description

The electric gun uses the energy initially stored in a capacitor bank to ohmically heat and explode a thin metallic bridge foil on a folded transmission line laminate. The explosion of the foil and the accompanying magnetic forces drive a thin plate of material down a barrel to impact on a target. The gun characteristics have been previously described.¹ Performance of the gun tends to be energy limited, with approximately 25% conversion efficiency from electrical to kinetic energy for larger, slower flyers (e.g., a 10-cm-square flyer weighing 4.3 g can be accelerated to approximately 3.2 km/s or a total kinetic energy of 22 kJ) down to approximately 8% for a 1-cm-square flyer at 18 km/s (with a total kinetic energy of just under 7 kJ).

1.2. Typical diagnostics

The environment of the gun during the foil acceleration process involves high currents and the possibility of

substantial EMI. Therefore, the diagnostics tend to be a combination of optical techniques, flash x-ray (FXR) snapshots, and reasonable soft recovery of the test specimen. The principal diagnostic instrument is a dual-beam Fabry-Perot velocimeter using an argon ion laser tuned for single-mode monochromatic operation. Velocity measurements to approximately 1% accuracy have been made for velocities over 1 km/s, and with reduced accuracy, velocities down to 10 m/s can be measured. The major secondary diagnostic tool is the dual-head FXR unit with selectable, independent timing of the two heads, if desired, to produce shadowgraph snapshots of debris images on an intensifier-enhanced film in an armored cassette. The third diagnostic instrument in general use is an electronic streaking camera that records light from a slit image to measure impact times and, with a suitable step flasher, shock speeds. We use a bucket filled with multilayer foam to catch the specimen in its final state, generally without appreciable damage from secondary impact with hard surfaces.

1.3. Experimental arrangement for flyer impact and shock-wave studies

Figure 1 shows an isometric cross-section of a laminate for the electric gun with a barrel and typical test specimen in place. In general, the test specimen is placed just outside of the muzzle to minimize the possible growth of any flyer-plate perturbations that could tend to reduce the planarity of the flat-plate impact (see Ref. 2 for an illustration of planarity of impact of a 0.38-mm-thick

*Work performed under the auspices of the U.S. Department of Energy by the Lawrence Livermore National Laboratory under Contract W-7405-Eng-48.

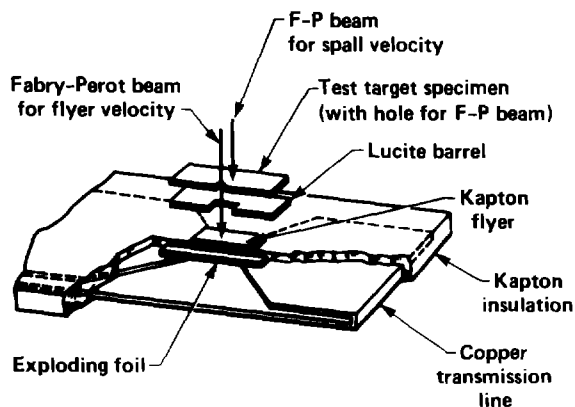


FIGURE 1
Exploded and cutaway view of a typical electric gun—configured for a spall experiment

Kapton flyer at 10.4 km/s), but far enough from the exploding foil region to avoid significant magnetic field effects from the high gun currents.

2. BASIC STRUCTURE OF SHOCK WAVES FOR THESE STUDIES

The structure of the shock pulse produced by flat-plate impact is important for understanding applications. We are confident of the relatively good integrity of the flyer on impact because the diagnostics for the electric gun include following the return beam of the Fabry-Perot from an intact, reflecting paint spot on the flyer until impact (or in some cases use of the electronic streak camera to check for flyer integrity on impact). Measurements and calculations are continuing to better characterize the decaying edge of the impact pulse including contributions from the accompanying aluminum plasma (the bridge foils used here were of 1100 Al) and decomposition products of the recoiling flyer.

2.1. Experimental shock-wave structure measurements

The structure of a shock wave produced by thin, flat-plate flyer impact is illustrated in Fig. 2. It shows the time record of the particle velocity U_p (measured with the Fabry-Perot velocimeter) at the impact interface for the case of a 0.3-mm-thick Kapton flyer impacting at 2.4 km/s on a 0.075-mm-thick layer of 6061-T6 Al backed by a 5-mm-thick LiF crystal. We consider this to yield a nominally 100-ns pulse. The 0.3-mm-thick Kapton flyer is constructed of two pieces each of 0.13-mm Kapton plus 0.02-mm adhesive, as can be seen in the pulse-shape de-

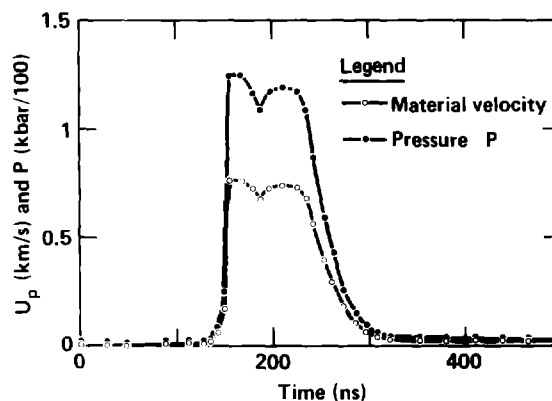


FIGURE 2
Pulse shape and amplitude calibration

tail of Fig. 2. Similar records have been made for a 0.254-mm-thick Mylar flyer and a 0.075-mm-thick Kapton flyer. Figure 2 includes a conversion of the U_p record to pressure using, as an approximation, the known linear U_p - U_s fit for the Hugoniot for LiF.

2.2. Range of flat-plate flyer capability

The shock-pulse duration available from electric-gun flyers varies from approximately 17 ns for 0.051-mm-thick Mylar flyers to over 400 ns for 1.27-mm-thick Lexon flyers; however, much of the recent data have been taken with 0.3-mm-thick Kapton flyers, as characterized in Fig. 2. Composite flyers incorporating a thin layer of Ta have also been used to produce even shorter high-pressure pulses. The incident impulse or momentum can readily be calculated, but the portion added from flyer recoil must be determined for a specific application because it depends upon the relative shock impedances of both the target and the flyer.

3. APPLICATIONS

3.1. Study of spall of 6061-T6 Al

Table 1(a) lists the qualitative variation of spall damage to 6.35-mm-thick samples of 6061-T6 Al for a range of incident impact momentum (per cm^2) for a 0.3-mm-thick Kapton flyer from below incipient spall to just above the threshold for free spall. Once the impact impulse is well above the threshold for free spall, the free-spall scab layer tends to carry away most of the forward momentum (typically 1.2 to 1.4 times the incident flyer momentum; the increase coming from flyer recoil and backward-traveling

debris). Table 1(b) lists the variation in spall with specimen thickness. For applications involving roughly 6.35-mm thickness of 6061-T6 Al, the attenuation of a 100-ns duration pulse is clearly important. The variation in threshold relative to the commonly quoted 7 to 7.5 ktaps for a 6.35-mm-thick target specimen shown in Table 1(a) is significant.

Table 1(c) lists the qualitative variation of spall near threshold for the impact case of a 0.075-mm-thick Kapton flyer (~ 25 -ns-pulse duration) on samples of 1.59-, 3.17-, 6.35-, and 9.53-mm-thick by 2.54-cm-wide by 10.16-cm-long strips of 6061-T6 Al assembled as a 10.16-by 10.16-cm target. It has been commonly argued that as

TABLE 1. Spall tests on 6061-T6 aluminum.*

(a) Test series to establish the threshold for free spall using a 0.3-mm-thick Kapton flyer incident on a 6.35-mm-thick sample of aluminum.

V_f (km/s)	0.6	0.9	1.3	1.5	1.6	1.9
I_i (ktaps)	2.6	3.9	5.6	6.5	6.9	8.2
Thickness						
6.35 mm	No damage	Minor I.S.	Mod. I.S.	Heavy I.S.	Heavy I.S.	Free spall

(b) Test series to explore the variation of the threshold for free spall with sample thickness using 0.3-mm-thick Kapton flyers.

V_f (km/s)	0.6	1.15	1.52
I_i (ktaps)	2.6	5.0	6.5
Thickness			
3.17 mm	No damage	Heavy I.S.	Free spall
6.35 mm	No damage	Mod. I.S.	Free spall
9.53 mm	No damage	No damage	Mod. I.S.

(c) Test series to explore the variation of the threshold for free spall with a shorter duration pulse using 0.075-mm-thick Kapton flyers.

V_f (km/s)	2.9	3.75	5.0
I_i (ktaps)	3.1	4.0	5.4
Thickness			
1.59 mm	Free spall	Free spall	Free spall
3.17 mm	Free spall	Free spall	Free spall
6.35 mm	Minor I.S.	Mod. I.S.	Free spall
9.53 mm	No damage	Minor I.S.	Free spall

*NOTE: V_f is the flyer velocity, I_i is the incident-flyer impulse, I.S. is incipient spall, and Mod. I.S. is moderate incipient spall.

long as the pulses were shorter than 1 μ s, only the delivered total impulse density counts. Our test results indicate that such an assumption is inaccurate, with appreciable reduction of the free-spall threshold (as compared to the 100-ns-pulse case) at least up to sample thicknesses greater than the 9.53-mm-thick 6061-T6 Al sample tested here. Figure 3 shows the FXR record for the 5-km/s-impact case of Table 1(c). Tests of the behavior of spall for flyer impact at oblique incidence show an increased threshold level for free spall and evidence of shredding of the spall scab into many fragments likely from lateral shear during the spall process.

4. NUMERICAL ANALYSIS

4.1. Uniform flyers impacting Al targets

The target response when impacted by 0.3-mm-thick Kapton flyers, one with normal incidence and one at 30° incidence, were computed using a 2-D Eulerian hydrocode. The initial velocity of the normal-incident flyer was 2.4 mm/ μ s, while the 30° incident flyer had an initial velocity of 6.0 mm/ μ s. The same code setup was used for both calculations, and both were run long enough to observe the initial spall-scab formation. For the normal incident flyer with a velocity of 2.4 mm/ μ s, only one spall scab is formed; the tensile wave remaining in the target after the initial spall is insufficient to produce



FIGURE 3

The FXR record for the case of the 5-km/s impact velocity column in Table 1(c). The x-ray shadowgraph was taken 75 μ s after flyer impact

more spall. Figure 4(a) shows the material boundaries of this calculation with velocity vectors just after the spall scab has formed. As shown by the velocity vectors, the spall has a much higher velocity than the target. Figure 4(b) is a density vs distance plot at $5.0 \mu\text{s}$ after initial impact showing the clean separation of the spall scab from the target. The pressure wave developed for the oblique incident flyer is seen in Fig. 4(c). The pressure-wave motion is initially in the same direction as the flyer motion, however, the release at the free surface is normal to the surface. The oblique incident flyer at $6\text{-mm}/\mu\text{s}$ velocity does couple sufficient energy into the target to produce spall. The calculation has not run long enough to fully characterize the spall, however, this initial spall is in good agreement with the experiments.

REFERENCES

1. J. E. Osher, H. H. Chau, G. R. Gathers, R. S. Lee, and R. C. Weingart, Application of a 100-kV electric gun for hypervelocity impact studies, in: 1986 Hypervelocity Impact Symp., San Antonio, Texas, October 21-24, 1986.
2. G. R. Gathers, J. E. Osher, H. H. Chau, R. C. Weingart, C. G. Lee, and E. Diaz, Release isentrope measurements with the LLNL electric gun, this volume.

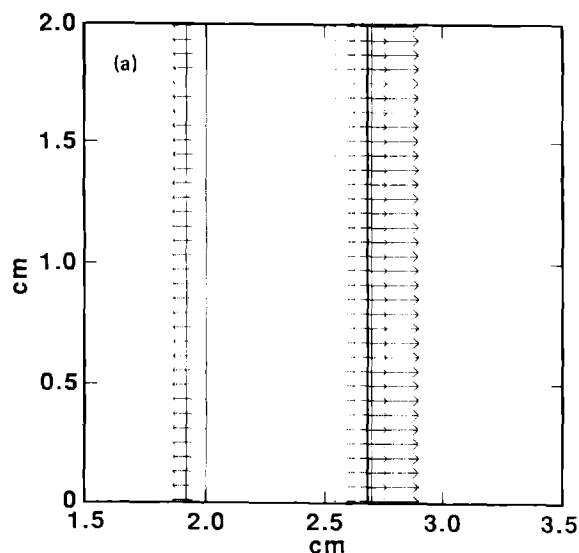


FIGURE 4(a)

At $1.4 \mu\text{s}$ after impact of a flyer at normal incidence, the spall scab is just starting to separate from the target material

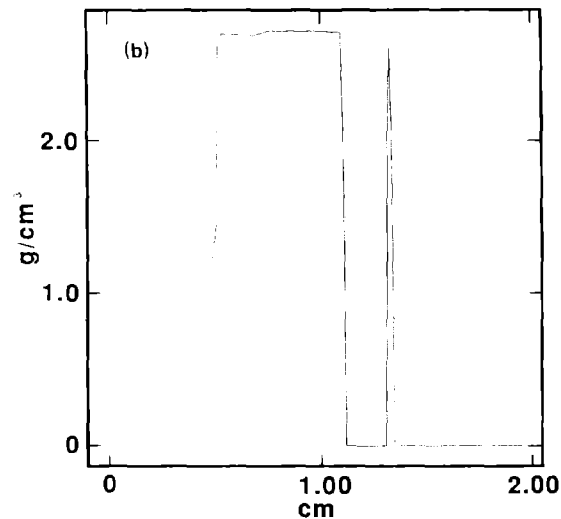


FIGURE 4(b)

At $5.0 \mu\text{s}$ after impact, the spall scab has separated from the target as an intact fragment

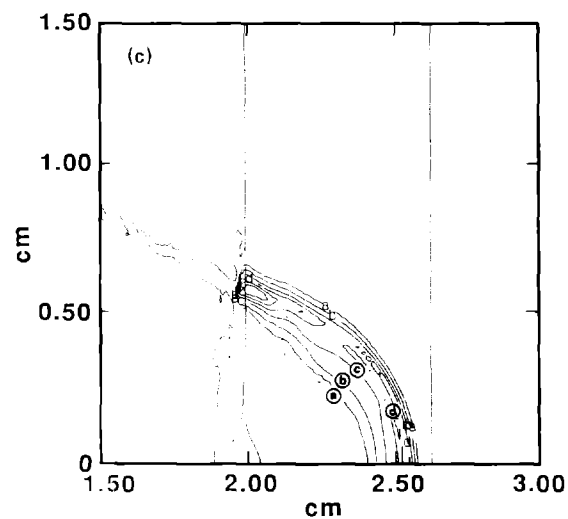


FIGURE 4(c)

The pressure contours at $t = 1.0 \mu\text{s}$ after impact for 30° incidence of a flyer on aluminum. The abscissa of the figure is normal to the aluminum surface. The peak pressure contours are: a = 5 kbar, b = 10 kbar, c = 20 kbar, and d = 30 kbar. Peak = 50 kbar